Springer

KSME

Journal of Mechanical Science and Technology 27 (4) (2013) 951~962
www.springerlink.com/content/1738-494x
DOI 10.1007/s12206-013-0206-8

Dynamic analysis of train-bridge system and riding comfort of trains with rail irregularities †

Khadri Youcef[1,2,*], Tekili Sabiha[1], Daya El Mostafa[2], Daouadji Ali[2] and Merzoug Bachir[1]

[1]*Mechanical Engineering Department, University of Badji Mokhtar, Laboratory LMI, Annaba, Algeria*
[2]*Université de Lorraine, LEM3-Metz, Ile du Saulcy, 57045 Metz, France*

(Manuscript Received March 3, 2012; Revised November 19, 2012; Accepted November 26, 2012)

Abstract

In this study, a modal superposition approach was adopted to derive the dynamic response of coupled vehicle and bridge systems. The train comprises a number of railway cars, each of which is modelled with ten degrees of freedom. The railway bridge was represented by a simply supported beam modelled as Euler-Bernoulli beam. In the numerical simulations, dynamic responses at the mid-span of the bridge and dynamic responses of the train under different train speeds are computed with random and non random rail irregularities. Effect of parameters like the depth and the position of the imperfection on the rail are taken into account. The coupled system of equations is integrated numerically by the newmark's β method. The results obtained show that the rail irregularities affect the vertical acceleration of the train, which serves as a measure of the riding comfort of the trains moving over a bridge.

Keywords: Dynamic train-bridge interaction; Rail irregularities; Riding comfort; Vehicle vibrations

1. Introduction

The dynamic of railway bridges under moving trains is important in the design of bridges and trains, and especially for high speed rail bridges. Three aspects need to be carefully taken into account in the analysis of the dynamic train-bridge system: the model of the bridge, the model of the train, and a good representation of rail irregularities. In the literature, the vehicle-bridge interaction problem is investigated using the beam models such as Euler-Bernoulli [1-4]. However, for the case when the cross section of the beam is relatively large in comparison with the beam span, the Timoshenko beam theory is employed by taking account of the effects of shear deformation and rotatory inertia in the analysis [4-6]. A general procedure for the dynamic response analysis of coupled vehicle and bridge systems using the modes superposition method is presented in Refs. [7-9] for a simply supported beam subject to a moving train. The moving load model is generally simple if only the bridge response is desired, such as a concentrated force [1, 2, and 5], moving mass model, which considers gravitational as well as inertial effects of the train [1, 2, 4], and spring-mass-damper system [1, 2, 10-12]. The train is modulated with two-wheel-set vehicles in Refs. [7, 11] and by two-stage suspension vehicles in Refs. [8, 13], where the model of a railway vehicle consisting of rigid bodies with lumped masses representing components such as axles. Using modal superposition technique, the semi- analytical methods [3, 13] are used for resolving the moving load problems. On the other hand, the dynamic response analysis for discrete system can be found using the finite elements method [11, 14, 15]. Yang et al. [14] also analyzed the dynamic response of the train-bridge system using finite elements method and newmark finite difference formula. Song [15] presented a new three-dimensional finite element in the analysis of high-speed train-bridge interactions. However, Cao [16] presented a semi-analytical/FEM model for dynamic analysis of the continuous girder bridge under high speed train. There are numerous publications on the dynamic behavior of the railway bridge under moving train, which employed the experimental method. One can mention the experiments of Ref. [17], where the dynamic responses of the bridge such as the deflections, the accelerations and the strains were measured by a laser velocity displacement transducer accelerometers and strain gauges, respectively. Zhang et al. [18] presented a numerical solution for the dynamic responses of a train-bridge interaction system subjected to multi-support seismic loads. And in Ref. [19] the experimental and numerical analysis of a composite bridge for high-speed trains is presented.

Track irregularities may be caused by factors such as small imperfections in materials, imperfections in manufacturing of rails and rail joints, terrain irregularities, and errors in survey-

*Corresponding author. Tel.: +213 772748 045, Fax.: +213 30821350
E-mail address: khadri152000@yahoo.fr
† Recommended by Editor Yeon June Kang

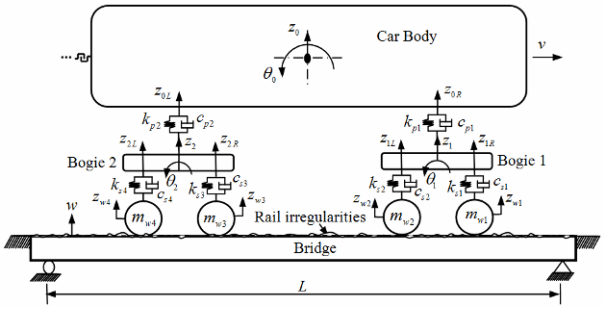

Fig. 1. Model of a railway vehicle.

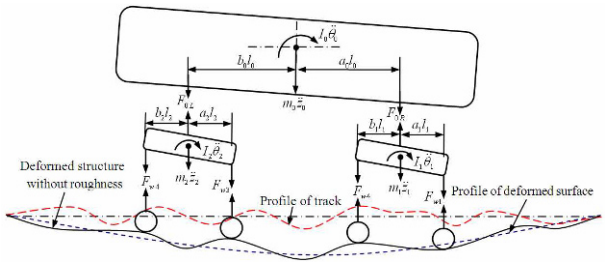

Fig. 2. The interaction forces between the vehicle of the train and bridge.

ing during design and construction. The track irregularities [10, 20, 21] are a second source of bridge vibrations, and a first source of train vibrations. Some research work on the effect of rail imperfections on the dynamic responses of the entire train and bridge coupling system has been performed. One must refer to the works of Ref. [7], this paper introduces an analytical procedure to derive equations of motion for the train-bridge interaction based on a modal superposition approach to investigate riding comfort of moving railway trains on bridges. To investigate the effect of track irregularity, we shall consider three classes of the random irregularity: Class 4, 5 and 6 and two cases of non-random irregularities: the first case represents the rail welds [22, 23] and the second case represents the corrugation wavelengths [24] on the rail surface. Other studies [25, 26] using Sperling's Ride Index for appreciating the riding comfort of the train. However, in Ref. [27], the Sperling's ride index is replaced by the standardized ISO, the riding comfort of trains running on a rationalized monorail bridge was estimated using 1/3 octave band spectral analysis based on ISO 2631 [28].

To carry out the analysis, the dynamic amplification factor (DAF), as the ratio of the maximum response resulting from moving loads, to the maximum static response, is calculated as the most important parameter in the bridge response. In addition to the DAF, dynamic responses of the train are evaluated in this study. A comfort index based on the vertical acceleration response of the train is used for evaluating the riding comfort of the train. Finally, the dynamic behavior of the bridge and of the train is carried out through a parametric study for various speeds, for the rail random irregularities i.e. rail roughness and non random irregularities with various depth and position of the imperfection on the bridge.

2. Dynamic model of a train-bridge interaction system

2.1 Vehicle model

The train can be modeled as several independent vehicle elements as shown in Fig. 1, and runs on the bridge at a constant speed. In studying a vehicle's vertical vibration, a ten degrees-of-freedom model is taken. Each vehicle element is composed of a car body, with a mass m_0 and mass moment of inertia I_0, two bogies, each one with a mass $m_{1,2}$ and mass moment of inertia $I_{1,2}$, four wheel-sets, each one with a mass m_{wk} (k = 1,4), and the connections between the components. The connections are characterized by the suspension system, which consists of springs and dampers with identical properties. The wheel-set and the bogie are connected by the primary suspension, while the car body is supported on the bogie through the secondary suspension. The system model adopts the following assumptions: (1) the springs in the vehicle elements are all with a linear property, and the dampers all with viscous property, (2) for the car body and bogies, vertical displacement and pitching motion is adopted, (3) the wheels are assumed to remain in contact with the rail at all times. The vertical displacement, velocity and acceleration of the wheel are, respectively, defined by:

$$z_{wk} = w_k(x_k,t) + r(x_k) = w_k + r_k,\ k = 1,4 \tag{1}$$

$$\dot{z}_{wk} = \dot{w}_k + v(w_k' + r_k'),\ k = 1,4 \tag{2}$$

$$\ddot{z}_{wk} = \ddot{w}_k + 2v\dot{w}_k' + v^2 w_k'' + v^2 r_k'',\ k = 1,4 \tag{3}$$

in which the dot represents differentiation with respect to time t; and the prime represents differentiation with respect to the abscissa x; v is the horizontal velocity of the moving vehicle; w_k is the bridge deflection; and r_k, are irregularities of the rail.

The interaction forces between the car body and the bogies are written as

$$F_{0R} = k_{p1}(z_{0R} - z_1) + c_{p1}(\dot{z}_{0R} - \dot{z}_1) \tag{4}$$

$$F_{0L} = k_{p2}(z_{0L} - z_2) + c_{p2}(\dot{z}_{0L} - \dot{z}_2)\,. \tag{5}$$

The interaction forces between the bogies and the wheel-set are written as

$$F_{w1} = k_{s1}(z_{1R} - z_{w1}) + c_{s1}(\dot{z}_{1R} - \dot{z}_{w1}) \tag{6a}$$

$$F_{w2} = k_{s2}(z_{1L} - z_{w2}) + c_{s2}(\dot{z}_{1L} - \dot{z}_{w2}) \tag{6b}$$

$$F_{w3} = k_{s3}(z_{2R} - z_{w3}) + c_{s3}(\dot{z}_{2R} - \dot{z}_{w3}) \tag{6c}$$

$$F_{w4} = k_{s4}(z_{2L} - z_{w4}) + c_{s4}(\dot{z}_{2L} - \dot{z}_{w4})\,. \tag{6d}$$

The internal forces and inertia forces of the car body, the bogies and the axles are shown in Fig. 2.

The dynamic equilibrium equations of the mass m_0 (car

body) are as follows:

$$m_0 b_0 l_0 \ddot{z}_0 + I_0 \ddot{\theta}_0 + F_{0R} l_0 = 0 \quad (7)$$

$$m_0 a_0 l_0 \ddot{z}_0 - I_0 \ddot{\theta}_0 + F_{0L} l_0 = 0 . \quad (8)$$

The dynamic equilibrium equations of the mass m_1 (bogie 1) are as follows:

$$m_1 b_1 l_1 \ddot{z}_1 - F_{0R} b_1 l_1 + I_1 \ddot{\theta}_1 + F_{w1} l_1 = 0 \quad (9)$$

$$m_1 a_1 l_1 \ddot{z}_1 - F_{0R} a_1 l_1 - I_1 \ddot{\theta}_1 + F_{w2} l_1 = 0 . \quad (10)$$

The dynamic equilibrium equations of the mass m_2 (bogie 2) are as follows:

$$m_2 b_2 l_2 \ddot{z}_2 - F_{0L} b_2 l_2 + I_2 \ddot{\theta}_2 + F_{w3} l_2 = 0 \quad (11)$$

$$m_2 a_2 l_2 \ddot{z}_2 - F_{0L} a_2 l_2 - I_2 \ddot{\theta}_2 + F_{w4} l_2 = 0 \quad (12)$$

where $a_i + b_i = 1$, $i = 0, 1, 2$ with a_i, and b_i are the coefficients of length.

By using the Eqs. (1)-(6) in the Eqs. (7)-(12), the coupling of the dynamic equations, we obtain the following:

$$[M_v]\{\ddot{z}_v\} + [C_v]\{\dot{z}_v\} + [K_v]\{z_v\} = \{F_v\} \quad (13)$$

where $[M_v]$, $[C_v]$, and $[K_v]$ are respectively, the mass, damping and stiffness matrices of the vehicle and $\{F\}$, is the interaction force vector applied on the vehicle; $\{z_v\} = \{z_{1R}, z_{1L}, z_{2R}, z_{2L}, z_{0R}, z_{0L}\}^T$, $\{\dot{z}_v\}$ and $\{\ddot{z}_v\}$ are respectively, displacement, velocity and acceleration vectors of the vehicle system. The expressions of the matrices and the vectors are given in appendix A.

The vertical and rotation displacements of the centers of gravity are given by

$$z_i = a_i z_{iL} + b_i z_{iR} \text{ and } \theta_i = (z_{iR} - z_{iL})/l_i, \; i = 0,1,2 . \quad (14)$$

2.2 Bridge model

The bridge subsystem is modeled as a uniform simply supported Euler-Bernoulli beams as shown in Fig. 1. The motion of the vehicle is defined by the wheels coordinates of the vehicle. With the vehicle moving from left to right, the longitudinal positions of the wheel of the vehicle are, respectively,

$$\begin{aligned} &x_1 = vt, \; x_2 = vt - l_1, \; x_3 = vt - a_1 l_1 - l_0 + a_2 l_2, \\ &x_4 = vt - a_1 l_1 - l_0 - b_2 l_2 . \end{aligned} \quad (15)$$

The equation of forced vibration for a bridge is obtained as

$$[M_b]\{\ddot{w}\} + [C_b]\{\dot{w}\} + [K_b]\{w\} = \sum_{k=1}^{nf} \delta_k \{F_{bk}\} \quad (16)$$

where $[M_b]$, $[C_b]$ and $[K_b]$ denote mass, damping and stiffness matrices of the bridge system, respectively. With, nf is the number of interaction forces, δ_k is Dirac function.

The force F_{bk} transferred to the bridge can be written as

$$F_{bk} = m_{wk} \ddot{z}_{wk} - F_{wk} + R_{wk} . \quad (17)$$

The static vehicular loads acting on the bridge are given by:

$$R_{w1} = (b_1(b_0 m_0 + m_1) + m_{w1}) g \quad (18a)$$

$$R_{w2} = (a_1(b_0 m_0 + m_1) + m_{w2}) g \quad (18b)$$

$$R_{w3} = (b_2(a_0 m_0 + m_2) + m_{w3}) g \quad (18c)$$

$$R_{w4} = (a_2(a_0 m_0 + m_2) + m_{w4}) g . \quad (18d)$$

Substituting the acceleration of the wheel $\ddot{z}_{wk}$ (Eq. (3)) into Eq. (17) yields:

$$F_{bk} = m_{wk}(\ddot{w}_k + 2v\dot{w}_k' + v^2 w_k'' + v^2 r_k'') - F_{wk} + R_{wk} . \quad (19)$$

By modal superposition and separation of variables, the deflection of the bridge can be expressed as

$$w(x,t) = \sum_{j=1}^{n} \phi_j(x) q_j(t) \quad (20)$$

where $\{q_j(t), j = 1,2,\ldots,n\}$ are the generalized coordinates, n is the number of the adopted vibration modes.

However the vibration modes are assumed by

$$\phi_j(x) = \sin(j\pi x / L) . \quad (21)$$

The coupling of Eqs. (13) and (16) gives a system containing the modal components of the bridge and the physical components of the vehicle:

$$\begin{bmatrix} M_{bb} & 0 \\ 0 & M_v \end{bmatrix} \begin{Bmatrix} \ddot{q} \\ \ddot{z}_v \end{Bmatrix} + \begin{bmatrix} C_{bb} & -\frac{2c_{sk}}{m_l L}\Phi^T \\ -c_{sk}\Phi & C_v \end{bmatrix} \begin{Bmatrix} \dot{q} \\ \dot{z}_v \end{Bmatrix} + \begin{bmatrix} K_{bb} & -\frac{2k_{sk}}{m_l L}\Phi^T \\ -k_{sk}\Phi - vc_{sk}\Phi' & K_v \end{bmatrix} \begin{Bmatrix} q \\ z_v \end{Bmatrix} = \begin{Bmatrix} F_{bb} \\ F_{vv} \end{Bmatrix} \quad (22)$$

where each sub-matrix of the matrices involved is given below:

$$M_{bb} = [I] + \frac{2}{m_l L} \sum_{k=1}^{nf} \phi_k^T m_{wk} \phi_k \quad (23a)$$

$$C_{bb} = diag[2\xi_j \omega_j] + \frac{2}{m_l L} \sum_{k=1}^{nf} \left(2v\phi_k^T m_{wk} \phi_k' + \phi_k^T c_{sk} \phi_k \right) \quad (23b)$$

$$K_{bb} = diag[\omega_j^2] + \frac{2}{m_l L} \sum_{k=1}^{nf} (v^2 \phi_k^T m_{wk} \phi_k'' + v\phi_k^T c_{sk} \phi_k' + \phi_k^T k_{sk} \phi_k) \quad (23c)$$

$$F_{bb} = -\left(2/m_l L\right)\sum_{k=1}^{nf}\left(R_{wk} + v^2 m_{wk} r_k'' + v c_{sk} r_k' + k_{sk} r_k\right)\phi_k^T \tag{23d}$$

$$F_{vv} = \begin{Bmatrix} vc_{s1}r_1' + k_{s1}r_1 \\ vc_{s2}r_2' + k_{s2}r_2 \\ vc_{s3}r_3' + k_{s3}r_3 \\ vc_{s4}r_4' + k_{s4}r_4 \\ 0 \\ 0 \end{Bmatrix} \tag{23e}$$

$$\phi_k = \begin{Bmatrix} \phi_1(x_k) & \phi_2(x_k) & \cdots & \phi_n(x_k) \end{Bmatrix}, \tag{23f}$$

$$\Phi = \begin{bmatrix} \phi_1(x_1) & \phi_2(x_1) & \cdots & \phi_n(x_1) \\ \phi_1(x_2) & \phi_2(x_2) & \cdots & \phi_n(x_2) \\ \phi_1(x_3) & \phi_2(x_3) & \cdots & \phi_n(x_3) \\ \phi_1(x_4) & \phi_2(x_4) & \cdots & \phi_n(x_4) \\ 0 & 0 & \cdots & 0 \\ 0 & 0 & \cdots & 0 \end{bmatrix} \tag{23g}$$

where m_l, E, I, ω_j and ξ_j are, respectively, the per-unit-length mass, the Young's modulus, the flexural moment of inertia, the jth undamped natural pulsation and modal damping ratio of the bridge.

The natural frequency of the beam is given by

$$\omega_j = \left(j\pi/L\right)^2 \sqrt{EI/m_l}\ . \tag{24}$$

The system of differential Eq. (22) can be solved with different integration techniques. In this study, the Eq. (22) are solved using implicit newmark integration scheme [29] and Δt = 2.5e-4 s. This method yields a stable and accurate solution, with Newmark's parameters $\gamma = 0.5$ and $\beta = 0.25$. A computer program in FORTRAN is developed for the analysis of railways defects on the dynamic response of a bridge.

Bridge response is defined in terms of the dynamic amplification factor (DAF), which is a ratio of the maximum response resulting from moving loads, to the maximum static response. The dynamic effects induced by the moving train on the railway bridge were investigated by computing the DAF, defined as

$$DAF = R_d(x)/R_s(x) \tag{25}$$

where $R_d(x)$ is the maximum dynamic displacement and $R_s(x)$ is the maximum static displacement (null speed) at the midspan of the bridge.

The dimensionless frequency parameter as $\alpha = f_v / f_b$ is defined as the ratio of the excitation frequency of the moving train, to the natural frequency of vibrations of the bridge. When f_v equals f_b (α = 1), the resonance of the bridge and trainload is very obvious. The critical speeds to resonate under the passage of the train are provided [30]:

$$v_{cr} = df_{bj}/k\,, j = 1,2,3,\ldots k = 1,2,3,\ldots, \tag{26}$$

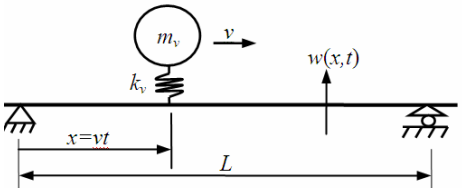

Fig. 3. Beam subjected to a moving mass-spring system.

where v is the train speed and d is the vehicle length.

The dynamic response of the bridge is estimated by superposition of the modes up to the 20th.

3. Validation

To validate the present algorithm, a simple example is considered (Fig. 3), which has been studied by several authors [31]. In these studies, the analytical solution of the interaction problem between a simply supported beam and a single degree of freedom (SDOF) moving mass-spring system (MS), where damping of the bridge and of the vehicle was ignored, as suggested in Ref. [2].

As shown in Fig. 3, a simple beam of span length L = 25 m is subjected to a moving mass-spring. The flowing data are adopted: Young's modulus E = 2.87 GPa; moment of inertia I = 2.90 m^4, mass per unit length m_l = 2303 kg/m, suspended mass m_v = 5750 kg, suspension stiffness k_v = 1595 kN/m, and speed v = 100 km/h (27.78 m/s). The results obtained are presented in Fig. 4 and compared to those obtained in Ref. [2]. From comparison, one can note that the present algorithm is in very good agreement with this reference.

4. Numerical study

This example serves to illustrate the effects of rail roughness and rail imperfections on the dynamic behavior of bridge and vehicle. Let us consider the train model, which is shown in Fig. 1, consisting of five identical vehicles (N_v = 5), traveling over a simply-supported bridge. The distance between the rear wheel of a vehicle and the front wheel of the following vehicle is 4 m. The data assumed below in Table 1 are close to those used in the case of high-speed train and railway bridges.

The first natural frequency of the bridge is f_b = 3.24 Hz. From Eq. (26), we obtain v_{cr1} = 77.80 m/s. Similarly, the second, the third, and the fourth speeds are v_{cr2} = 38.9 m/s, v_{cr3} = 25.93 m/s, and v_{cr4} = 19.45 m/s.

4.1 Effects of random irregularities

The rail irregularities are a second source of bridge vibrations, and a first source of train vibrations. Rail irregularities can be divided into random and non-random irregularities. The roughness of the rails is included in the category of random irregularities. The sample of rail irregularities can be produced by inverse Fourier transform shown as follows:

Table 1. Parameters of the vehicle, and of the bridge.

Mass of car body (t)	41.75
Mass of bogie (t)	3.04
Mass of wheel (t)	1.7
Mass moment of inertia of car body (t-m^2)	2086
Mass moment of inertia of bogie (t-m^2)	3.93
Stiffness of primary suspension system (kN/m)	530
Stiffness of secondary suspension system (kN/m)	1180
Damping of primary suspension system (kN-s/m)	90.2
Damping of secondary suspension system (kN-s/m)	39.2
Distance between centers of gravity of bogies (m)	17.5
Distance between two centers of axles (m)	2.5
Length of the vehicle (m)	24
Coefficients of length	0.5
Young's modulus of the bridge (GPa)	200
Per-unit-length mass (t/m)	10
Flexural moment of inertia (m^4)	0.17238
Damping coefficient (%)	2.5
Length of bridge unit (m)	30
Mass of car body (t)	41.75
Mass of bogie (t)	3.04

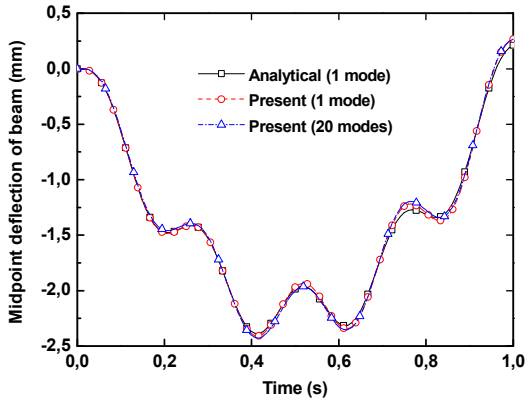

(a) Midpoint deflection of beam

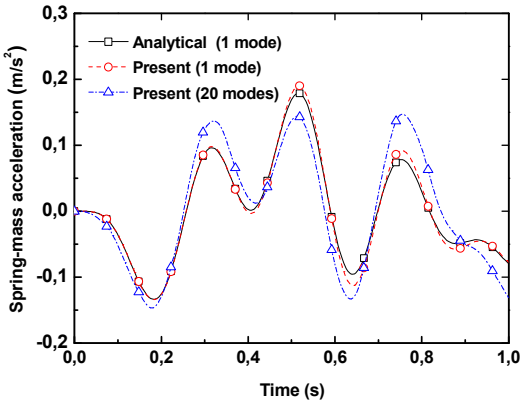

(b) Acceleration of spring-mass

Fig. 4. The dynamic response of the beam and spring-mass.

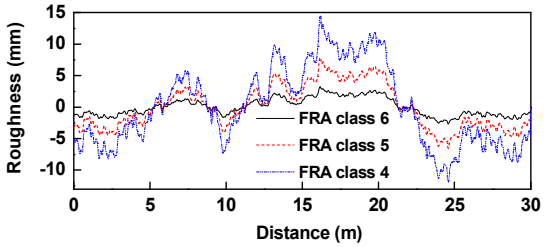

Fig. 5. Profiles for three classes of railway track quality.

$$r(x)=\sum_{k=1}^{N}\sqrt{4A_r\left(\omega_{sk}/\omega_{s0}\right)^{-2}\Delta\omega}\cos\left(\omega_{sk}x-\varphi_k\right) \tag{27}$$

where A_r is the magnitude parameter (m^3/cycle), $\omega_{s0} = 1/(2\pi)$, the frequency of discontinuity (cycle/m), $\omega_{sk} = k.\Delta\omega$, the number of waves (cycle/m), it is the frequency within the interval $[\omega_{min}, \omega_{max}]$, the frequency increment is defined as $\Delta\omega = 2\pi/(N\lambda_c)$, $\lambda_c = 2L$, L is the length of the bridge, N is the total number of terms used to determine the rail surface roughness and x is the position measured from the left end of bridge. Introducing the last expressions in Eq. (27), from where:

$$r(x)=\sum_{k=1}^{N}\sqrt{4A_r\left(\frac{2k\pi}{\lambda_c\omega_{s0}}\right)^{-2}\frac{2\pi}{\lambda_c}}\cos\left(\omega_{sk}x-\varphi_k\right). \tag{28}$$

By using FFT algorithm with Monte Carlo simulation to generate a random number φ_k uniformly distributed between 0 and 2π [32]. The railway track quality is categorized into classes ranging from the poorest in class 1 to the finest in class 6 designated by the federal railroad administration (FRA), USA. To investigate the effect of track irregularity, we shall consider three classes of track irregularity: class 4, class 5 and class 6. For track class 4, the route frequency parameters are ω_{min} = 0.0233 (cycle/m) and ω_{max} = 0.131 (cycle/m) and the value of the spectral roughness coefficient is $A_r = 2.75 \times 10^{-8}$ (m^3/cycle) [33]. For the other classes of track irregularity, i.e. classes 5 and 6 are generated accordingly by proportion. The irregular profiles $r(x)$ of the three classes of tracks are computed with N = 180 and plotted in Fig. 5. In this study the frequency increment is defined as $\Delta\omega = 2\pi/(N \times \lambda_c) = 2\pi/(180 \times 2 \times 30) = 5.81\text{e-}4$ (cycle/m). Then in Ref. [1] the frequency increment is given by $\Delta\omega = (\omega_{max} - \omega_{min})/N = (0.131 - 0.0233)/180 = 5.9\text{e-}4$ (cycle/m), the result is the same.

To carry out the analysis, the computations of the dynamic amplification factor (DAF) are made in the interval [0, 90 m/s] with a step of 5 m/s. Fig. 6 shows the dynamic amplificatory factor as a function of the speed for the smooth track and with tree different classes of track irregularity. The dynamic amplification factor increases as the train speed increases and reaches its maximum at v = 77.5 m/s which coincides very well with critical speed (v_{cr1} = 77.8 m/s) predicted by the formula (26). For bridge subjected to high-speed trains, the excessive vibration occurs due to resonance phenomenon. Also, from

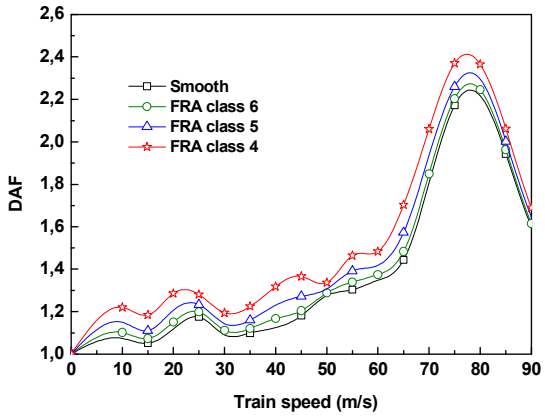

Fig. 6. DAF of bridge at mid-span under three classes of track irregularity.

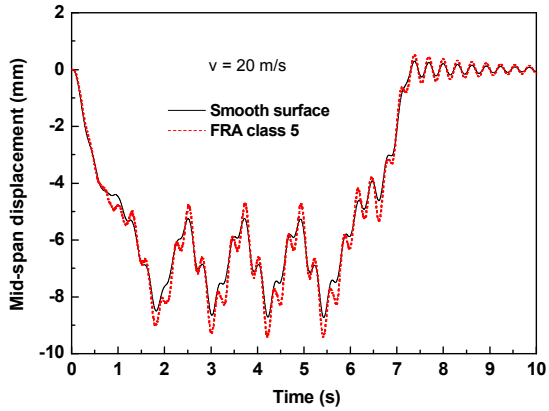

Fig. 7. Mid-span deflection versus time t for a bridge with and without rail roughness (train speed v = 20 m/s).

Fig. 6, we notice that the differences between the two cases Smooth and FRA class 6 are slight. On the other hand for the two other cases, one notes that the difference is more significant and almost independent the speed of the train. The random irregularities lead to a little increase of the dynamic amplification factor for FRA classes 4, 5, and 6 of about 0.89%, 3.11%, 7.11%, respectively.

The time history deflection of the midpoint of the bridge with and without rail roughness (FRA class 5) has been plotted in Fig. 7 for v_{cr4} = 20 m/s. As shown in this figure, the rail roughness FRA class 5 has little effect on the vertical displacement of the bridge. The random irregularities affect little the dynamic responses of the bridge.

The vertical displacement, rotation displacement, vertical acceleration and rotation acceleration of the first vehicle body versus time t with and without rail roughness (FRA class 5) with v = 20 m/s are shown in Figs. 8(a)-(d) respectively.

As shows in Figs. 8, the rail roughness FRA class 5 affects the dynamic response of the train. The riding comfort of trains is a parameter of great importance for the vehicles, especially for high-speed trains. The accelerations response of the train serves as a measure of the riding comfort. The maximum ver-

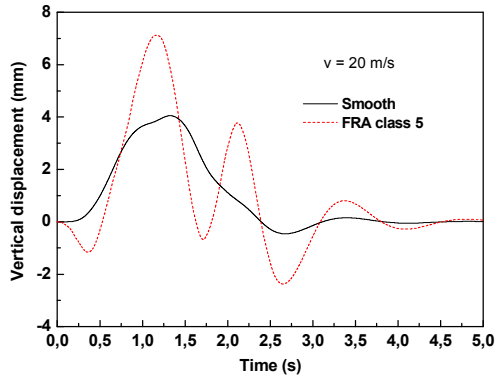

(a) Vertical displacement

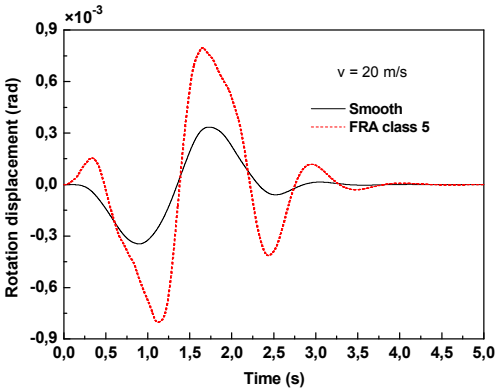

(b) Rotation displacement

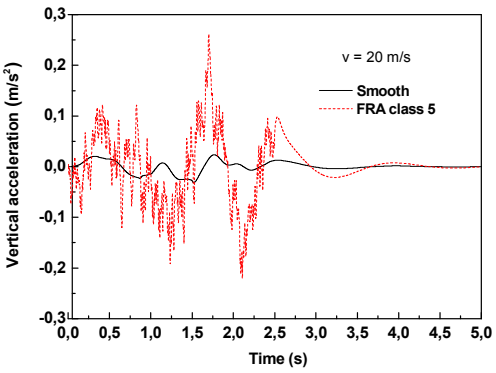

(c) Vertical acceleration

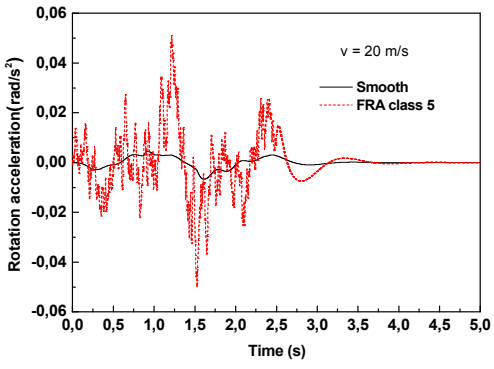

(d) Rotation acceleration

Fig. 8. Dynamic responses of the train with and without rail roughness (train speed v = 20 m/s).

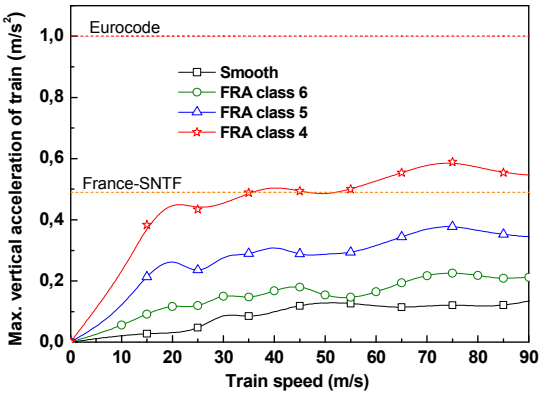

Fig. 9. Maximum vertical acceleration of the train for three classes FRA class 4, 5 and 6.

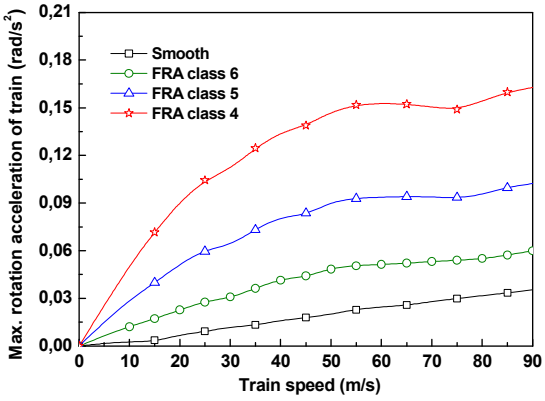

Fig. 10. Maximum rotation acceleration of the train for three classes FRA class 4, 5 and 6.

tical accelerations of the train for the three classes of track irregularity under different train speeds have been plotted in Fig. 9.

Only the case FRA class 4 exceed the tolerance limit of 0.49 m/s^2 (= 0.05 g) tentatively adopted by the Taiwan high speed rails [33] and France-SNCF [34] concerning passengers' riding comfort. The maximum vertical acceleration of the train moving over irregular tracks of the class 4 reaches the limit value a = 0.6 m/s^2 at train speed v = 75 m/s which is almost coincident with v_{cr1} = 77.78 m/s.

The vertical acceleration of the train is significantly affected by the rail roughness. It remains nearly independent of the train speed in the moderate to high speed range. The estimated asymptotic values for FRA classes 4, 5, 6 and smooth are 0.6, 0.4, 0.3 and 0.2 m/s^2, respectively. Then for the less strict limit of 1.0 m/s^2 suggested by Eurocode [35], all classes of track irregularity are acceptable (Fig. 9).

Maximum rotation acceleration of the train is presented in Fig. 10 for the three different classes of track quality, which shows a trend of increase for higher train speeds. The rotation acceleration of the train increases with a lower railway track quality and it is proportional to the magnitude of the roughness.

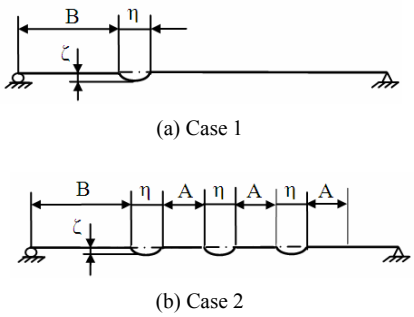

Fig. 11. Cases of the non-random irregularities.

The effect of rail irregularities is generally small on the bridge response, i.e. bridge dynamic displacement and DAF. However, it can affect drastically the rotation acceleration and vertical acceleration of the train. The reason for this is that the exciting frequencies induced by track irregularities are filtered out by the suspension system of vehicle in transmission to the car body.

4.2 Effects of non-random irregularities

The non-random irregularities on the rail surface can be classified in two categories: periodic and discrete irregularities. The non-random irregularities can be mathematically expressed by the following function, which is used in Ref. [33]:

$$r_d(x) = \frac{1}{2}\zeta\left(1-\cos 2\pi x/\eta\right). \tag{29}$$

For a series of non-random irregularities, we obtain the following:

$$r_d(x) = \begin{cases} \dfrac{1}{2}\zeta\left(1-\cos\left(\dfrac{2\pi(x-C)}{\eta}\right)\right), & for\ C \le x \le C+\eta \\ 0, & elsewhere, \end{cases} \tag{30}$$

where

$$C = B + k(A+\eta), \quad k = 0,1,\ldots,N_i \tag{31}$$

and

$$N_i = (L-B)/(A+\eta). \tag{32}$$

N_j is the imperfection number, ζ, η denote the depth and length of the imperfection, respectively, A is the rail length between two imperfections, B is the distance from the origin to the first imperfection.

The non-random irregularities exist in a number of different forms. Two cases of non-random irregularities that are often observed in practice are considered in this study (Fig. 11) in order to analyze their effects on the dynamic behavior of the bridge and of the train. The first case represents the discrete

Table 2. The non-random irregularities parameters.

	Case 1	Case 2
A (m)	0	5
B (m)	12.5	0
ζ (m)	0.005	0.005
η (m)	5	5
Ni	1	3

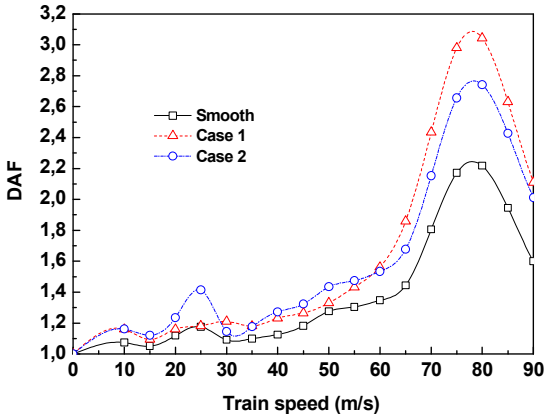

Fig. 12. DAF of bridge at mid-span for cases 1 and 2.

irregularities, as possible rail welds or corrugation, Fig. 11(a); the weld geometry is dominated by an irregularity with a longer length-scale and has a very bad quality. The second case represents the corrugation wavelengths (periodic irregularities) on the rail surface that can be caused by a phenomenon of fatigue of the rail due to dynamic behavior of the track, Fig. 11(b).

The non-random irregularities parameters of Fig. 11 are reported in Table 2. For case 1 if $B = (L-\eta)/2 = 12.5$ m, i.e., the imperfection of the rail is located at the mid-span of bridge. However, for case 2, the imperfection of the rail is located at $B = 0$ m.

In Fig. 12, we assumed that the velocity of the train increases from 0 to 90 m/s with an increment of 5 m/s. This shows the DAF versus speed for the perfect track and with different cases of the non-random irregularities (cases 1 and 2).

As can be seen from Fig. 12 for case 1 and 2, the introduction of non-random irregularities on rail significantly increases the dynamic response of the bridge (DAF) and particularly around the peak response caused by the resonance. Which is true for a great range of vehicle speeds (more than 60 m/s) representing a moderate to high vehicle speed.

Fig. 13 shows the time history of the bridge deflection with and without non-random irregularities for cases 1 and 2, with $v = 80$ m/s near the critical speed ($v_{cr1} = 77.8$ m/s). As shown in Fig. 13 the non-random irregularities lead to an increase of the maximum vertical displacement of bridge for cases 1 and 2 of about 37.23%, 23.87% , respectively.

The vertical displacement, vertical acceleration, rotation

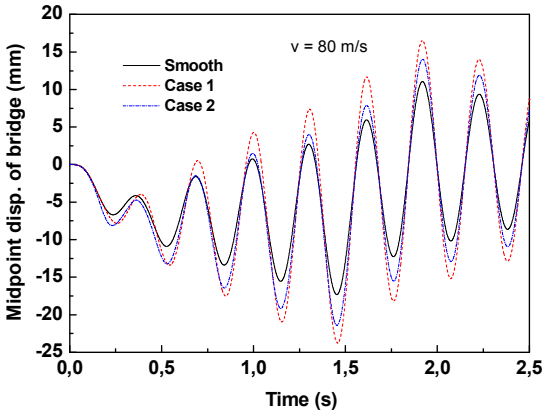

Fig. 13. Mid-span deflection of the bridge versus time t for cases 1 and 2 (train speed $v = 80$ m/s).

displacement and rotation acceleration of train versus time t for two cases 1 and 2 with $v = 80$ m/s are shown in Figs. 14(a)-(d), respectively. The moments of entry of the wheels 1, 2, 3 and 4 in the rail imperfection are 0.156 s, 0.187 s, 0.375 s and 0.406 s, respectively, as shown in Figs. 14(c) and 14(d). Figs. 14 shows the sensitivity of the dynamic response of the train due to the presence of the non-random irregularities particularly of the vertical acceleration. The vertical acceleration of the train has a significant variation when the vehicle arrives at the position of non-random irregularities, as shown in Fig. 14(c). It should be noted that the acceleration of the car body has been taken as a measure of the passenger's riding comfort.

The effect of the imperfection depth (ζ) on the maximum vertical acceleration of the train for cases 1 and 2 under different train speeds (0 to 130 m/s) is plotted in Figs. 15(a) and 15(b), respectively. The vehicles on the structure increased the unit mass and generally lowered the natural frequencies of vibration and decrease the impact. The maximum vertical accelerations of the train shown in Figs. 15(a) and 15(b) tend to increase when ζ is augmented. It generally increases as the train speed increases. The non-random irregularities have a considerable effect on train vertical acceleration for high speeds (more than 40 m/s) representing a moderate to high speed train for cases 1 and 2.

It is interesting to note that, for low speeds (less than 40 m/s) the effect of the non-random irregularities on vertical acceleration of the train is smaller Fig. 15(a) (case 1). One notes that the allowable maximum vertical acceleration of 0.49 m/s^2 recommended by France-SNCF was exceeded only when $\zeta = 10$ mm, in the case 1 for the train speed more than 70 m/s (Fig. 15(a)) and in the case 2 for the train speed more than 45 m/s (Fig. 15(b)).This is certainly harmful if the riding comfort of the train is concerned. Then for the less strict limit of 1.0 m/s^2 suggested by Eurocode [35], all cases are acceptable.

To investigate the influence of the distance B on the vertical acceleration of the train, nineteen different values of B are used.

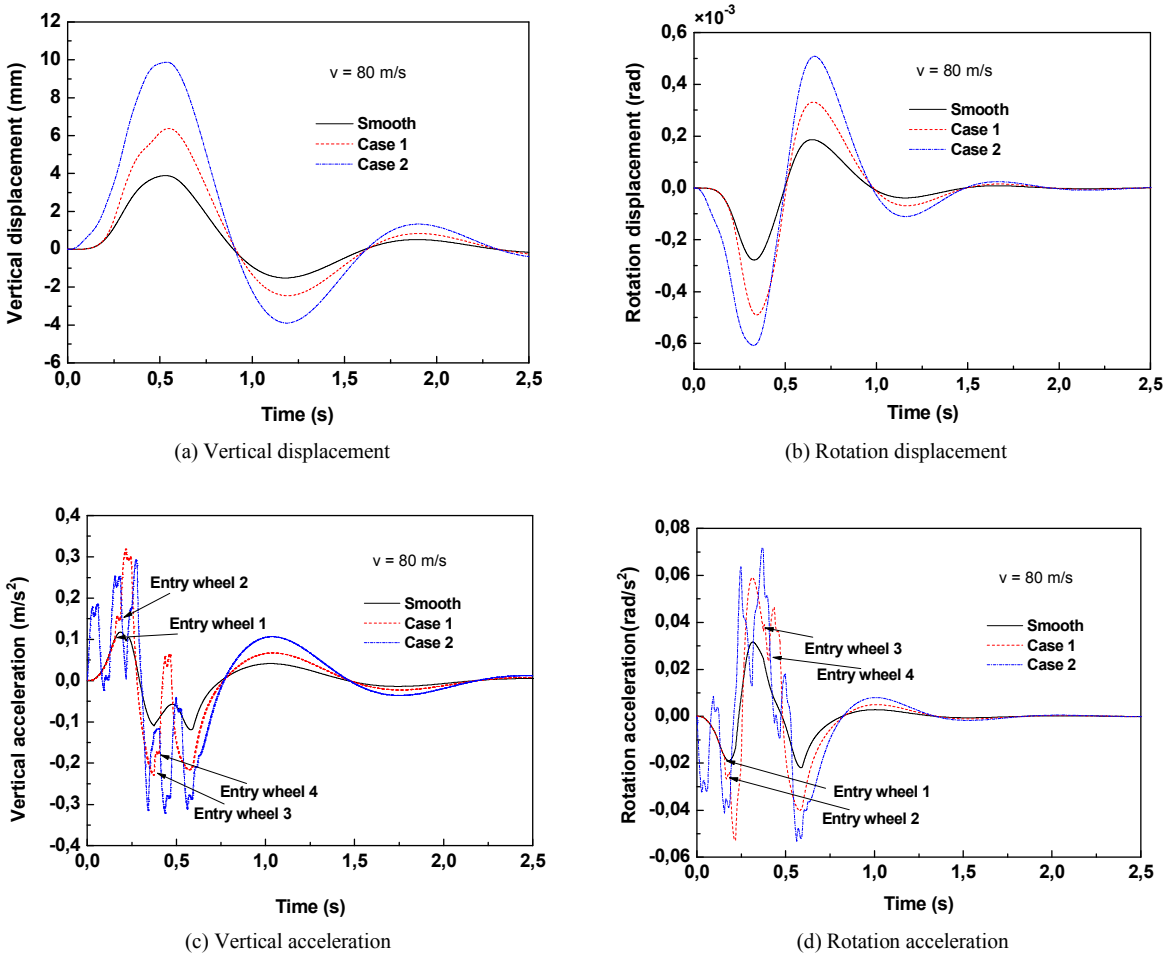

(a) Vertical displacement (b) Rotation displacement

(c) Vertical acceleration (d) Rotation acceleration

Fig. 14. Dynamic responses of the train for cases 1 and 2 with train speed v = 80 m/s.

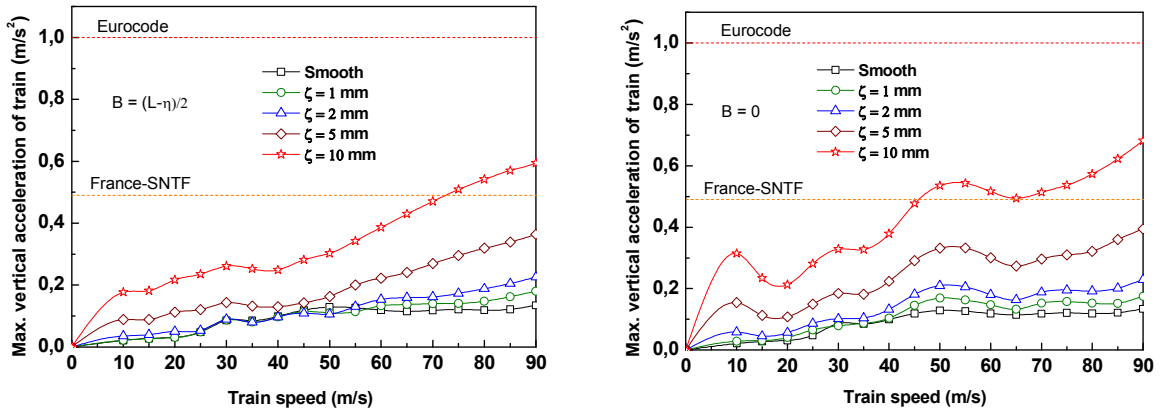

(a) Case 1 (b) Case 2

Fig. 15. The comparison of the effect of ζ on the vertical acceleration of the train for cases 1 and 2 under different train speeds.

The value of B is calculated as follows:

$$B = i_B \times L/30, \quad i_B = 1,2,\ldots,N_B \tag{33}$$

where N_B is the number of B values.

Fig. 16 shows the effect of B on the vertical acceleration of the train for case 1 under different values of ζ and with v = 80 m/s. The maximum vertical acceleration of the train is 0.58 m/s^2 for B = 11 m and 16 m. However, if the imperfection is located at mid-span B = (L-η)/2 = 12.5 m, the vertical accel-

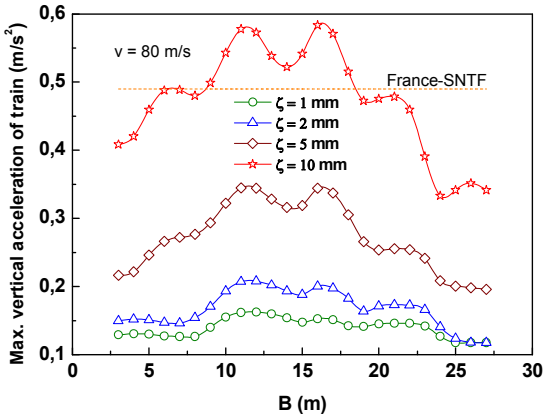

Fig. 16. The effect of B on the vertical acceleration of the train for case 1 under different values of ζ.

eration of the train is only 0.54 m/s^2. It is obvious, since the optimal dynamic response is not forcing in the medium of the beam like the case of the static response. In general, the position of the imperfection corresponding to the maximum value of the vertical acceleration of the train is around the mid-span of bridge.

5. Conclusions

The dynamic responses of the railway bridge and of the train are investigated by a modal superposition method. The riding comfort which is a key factor in the design of the high speed train is evaluated by the vertical acceleration of the car body. The following conclusions can be drawn from this study:

(1) The critical speed for resonance solved by the present method coincides very well with that predicted using Eq. (26) derived in Ref. [30]. For bridge subjected to high-speed trains, the excessive vibration occurs due to resonance phenomenon.

(2) The presence of the rail random irregularities affects little the responses of the bridge. However, it can affect considerably the dynamic responses of the train, i.e. the rotation acceleration and vertical acceleration, which can be harmful for the riding comfort of the train. The vertical acceleration remains nearly independent of the train speed in the moderate to high speed range (more than 40 m/s).

(3) The introduction of non-random irregularities on the rail significantly increases the dynamic response of the bridge (DAF) and particularly around the peak response caused by the resonance.

(4) The dynamic responses of the train are very sensitive to the non-random irregularities; it tends to increase when depth of the imperfection (ζ) is augmented and it increases as the train speed increases. The vertical acceleration has significant variation when the vehicle arrives at the position of non-random irregularities. This fact is certainly harmful for the passenger's riding comfort of the trains.

(5) In general, the dynamic vertical acceleration of the train attains its maximum value when the imperfection is located around the mid-span of bridge. Therefore, maintaining a smooth track surface in railway engineering is very important.

Nomenclature

m_0 : Mass of car body
$m_{1,2}$: Mass of bogie
m_{wk} : Mass of wheel
I_0 : Mass moment of inertia of car body
$I_{1,2}$: Mass moment of inertia of bogie
$k_{p1,2}$: Stiffness of primary suspension system
k_{sk} : Stiffness of secondary suspension system
$c_{p1,2}$: Damping of primary suspension system
c_{sk} : Damping of secondary suspension system
l_0 : Distance between centers of gravity of bogies
$l_{1,2}$: Distance between two centers of axles
d : Length of the vehicle
a_i, b_i : Coefficients of length
E_b : Young's modulus of the bridge
m_b : Per-unit-length mass
I_b : Flexural moment of inertia
ξ : Damping coefficient of the bridge
L : Length of bridge unit

References

[1] L. Frýba, *Vibration of solids and structures under moving loads*, Thomas Telford Ltd., London (1999).
[2] J. M. Biggs, *Introduction to structural dynamics*, New York (NY, USA): McGraw-Hill (1964).
[3] A. E. Martinez-Castro, P. Museros and A. Castillo-Linares, Semi-analytic solution in the time domain for non-uniform multi-span Bernoulli-Euler beams traversed by moving loads, *Journal of Sound and Vibration*, 294 (1-2) (2006) 278-97.
[4] M. Simsek, Vibration analysis of a functionally graded beam under a moving mass by using different beam theories, *Composite Structures*, 92 (4) (2010) 904-17.
[5] R. T. Wang, Vibration of multi-span Timoshenko beams to a moving force, *Journal of Sound and Vibration*, 207 (5) (1997) 731-742.
[6] J. S. Wu and L. K. Chiangn, Out-of-plane responses of a circular curved Timoshenko beam due to a moving load, *International Journal of Solids and Structures*, 40 (2003) 7425-7448.
[7] P. Lou, Vertical dynamic responses of a simply supported bridge subjected to a moving train with two wheel-set vehicles using modal analysis method, *International Journal for Numerical Methods in Engineering*, 64 (9) (2005) 1207-1235.
[8] P. Lou, G. L. Dai and Q. Y. Zeng, Modal coordinate formulations for a simply supported bridge subjected to a moving train modelled as two-stage suspension vehicles, *Proceedings of the Institution of Mechanical Engineers Part C Journal of Mechanical Engineering Science*, 219 (10) (2005) 1027-1040.
[9] Y. L. Xu., Q. Li, D. J. Wu and Z. W. Chen, Stress and accel-

eration analysis of coupled vehicle and long-span bridge systems using the mode superposition method, *Engineering Structures*, 32 (2010) 1356 -1368.

[10] K. C. Chang, F. B. Wu and Y. B. Yang, Disk model for wheels moving over highway bridges with rough surfaces, *Journal of Sound and Vibration*, 330 (2011) 4930-4944.

[11] H. Azimi, K. Galal and O. A. Pekau, A modified numerical VBI element for vehicles with constant velocity including road irregularities, *Engineering Structures*, 33 (2011) 2212-2220.

[12] J. D. Yau, Y. B. Yang and S. R. Kuo, Impact response of high speed rail bridges and riding comfort of rail cars, *Engineering Structures*, 21 (1999) 836-844.

[13] X. W. Liu, J. Xie, C. Wu and X. C. Huang, Semi-analytical solution of vehicle-bridge interaction on transient jump of wheel, *Engineering Structures*, 30 (9) (2008) 2401-2412.

[14] Y. B. Yang and J. D. Yau, Vehicle-bridge interaction element for dynamic analysis, *J Struct Eng ASCE*, 123 (1997) 1512-8.

[15] M. K. Song, H. C. Noh and C. K. Choi, A new three-dimensional finite element analysis model of high-speed train-bridge interactions, *Engineering Structures*, 25 (13) (2003) 1611-1626.

[16] Y. Cao, H. Xia and Z. Li, A semi-analytical/FEM model for predicting ground vibrations induced by high-speed train through continuous girder bridge, *Journal of Mechanical Science and Technology*, 26 (8) (2012) 2485-2496.

[17] H. Xia, G. D. Roeck, N. Zhang and J. Maeck, Experimental analysis of a high-speed railway bridge under Thalys trains, *Journal of Sound and Vibration*, 268 (2003) 103-113.

[18] N. Zhang, H. Xia and G. D. Roeck, Dynamic analysis of a train-bridge system under multi-support seismic excitations, *Journal of Mechanical Science and Technology*, 24 (11) (2010) 2181-2188.

[19] K. Liu, E. Reynders, G. D. Roeck and G. Lombaert, Experimental and numerical analysis of a composite bridge for high-speed trains, *Journal of Sound and Vibration*, 320 (1-2) (2009) 201-220.

[20] X. Lei and N. A. Noda, Analyses of dynamic response of vehicle and track coupling system with random irregularity of track vertical profile, *Journal of Sound and Vibration*, 258 (1) (2002) 147-65.

[21] H. Honda, Y. Kajikawa and T. Kobori, Spectra of road surface roughness on bridges, *Journal of Structural Division*, ASCE, 108 (ST9) (1982) 1956-1966.

[22] W. Cai, Z. Wen, X. Jin and W. Zhai, Dynamic stress analysis of rail joint with height difference defect using finite element method, *Engineering Failure Analysis*, 14 (2007) 1488-1499.

[23] E. Kabo, J. C. O. Nielsen and A. Ekberg, Prediction of dynamic train-track interaction and subsequent material deterioration in the presence of insulated rail joints, *Vehicle System Dynamics*, 44 (2006) 718-729.

[24] T. X. Wu and D. J. Thompson, An investigation into rail corrugation due to micro-slip under multiple wheel-rail interactions, *Wear*, 258 (2005) 1115-1125.

[25] Y. G. Kim, H. B. Kwon, S. W. Kim, C. K. Park and T. W. Park, Correlation of ride comfort evaluation methods for railway vehicles, Proc. IMech F, *J. Rail and Rapid Transit*, 217 (2) (2003) 73-88.

[26] Y. S. Wu and Y. B. Yang, Steady-state response and riding comfort of trains moving over a series of simply supported bridges, *Engineering Structures*, 25 (2003) 251-265.

[27] C. H. Lee, C. W. Kim, M. Kawatani, N. Nishimura and T. Kamizono, Dynamic response analysis of monorail bridges under moving trains and riding comfort of trains, *Engineering Structures*, 27 (2005) 1999-2013.

[28] ISO 2631/2. Evaluation of human exposure to whole-body vibration- Part 2: Continuous and shock-induced vibration in buildings (1 to 80 Hz) (1989).

[29] N. M. Newmark, A Method of computation for structural dynamics, ASCE, *Journal of Engineering Mechanics Division*, 85 (EM3) (1970) 67-94.

[30] L. Frýba, A rough assessment of railway bridges for high speed trains, *Engineering Structures*, 23 (5) (2001) 548-556.

[31] Y. B. Yang and J. D. Yau, Vehicle-bridge interaction element for dynamic analysis, *Journal of Structural Engineering*, ASCE, 123 (11) (1997) 1512-1518.

[32] W. H. Press and S. H. Teukolsky, Portable random number generators, *Computers in Physics*, 6 (1992) 522-524.

[33] Y. B. Yang, J. D. Yau and Y. S. Wu, *Vehicle-Bridge interaction dynamics with applications to high-speed railways*, World scientific publishing Co Pte Ltd., Singapore (2004).

[34] J. Grandi and P. Ramondenc, *The dynamic behavior of railways on high speed lines*, SNCF, France (1990).

[35] European Committee for Standardization, EUROCODE 1: basis of design and actions on structures, part 3: traffic loads on bridges, ENV 1991-3, (1995).

Appendix A

The mass, damping and stiffness matrices of the vehicle are respectively:

$$[M_v]=\begin{bmatrix} m_1b_1^2+\frac{I_1}{l_1^2} & m_1b_1a_1-\frac{I_1}{l_1^2} & 0 & 0 & 0 & 0 \\ & m_1a_1^2+\frac{I_1}{l_1^2} & 0 & 0 & 0 & 0 \\ & & m_2b_2^2+\frac{I_2}{l_2^2} & m_2b_2a_2-\frac{I_2}{l_2^2} & 0 & 0 \\ & & & m_2a_2^2+\frac{I_2}{l_2^2} & 0 & 0 \\ & sym. & & & m_0b_0^2+\frac{I_0}{l_0^2} & m_0b_0a_0-\frac{I_0}{l_0^2} \\ & & & & & m_0a_0^2+\frac{I_0}{l_0^2} \end{bmatrix} \quad \text{(A1)}$$

$$[C_v]=\begin{bmatrix} c_{s1}+c_{p1}b_1^2 & c_{p1}a_1b_1 & 0 & 0 & & 0 \\ & c_{s2}+c_{p1}a_1^2 & 0 & 0 & -c_{p1}a_1 & 0 \\ & & c_{s3}+c_{p2}b_2^2 & c_{p2}a_2b_2 & 0 & -c_{p2}b_2 \\ & & & c_{s4}+c_{p2}a_2^2 & 0 & -c_{p2}a_2 \\ & sym. & & & c_{p1} & 0 \\ & & & & & c_{p2} \end{bmatrix} \quad \text{(A2)}$$

$$[K_v]=\begin{bmatrix} k_{s1}+k_{p1}b_1^2 & k_{p1}a_1b_1 & 0 & 0 & -k_{p1}b_1 & 0 \\ & k_{s2}+k_{p1}a_1^2 & 0 & 0 & -k_{p1}a_1 & 0 \\ & & k_{s3}+k_{p2}b_2^2 & k_{p2}a_2b_2 & 0 & -k_{p2}b_2 \\ & & & k_{s4}+k_{p2}a_2^2 & 0 & -k_{p2}a_2 \\ & & sym. & & k_{p1} & 0 \\ & & & & & k_{p2} \end{bmatrix} \quad \text{(A3)}$$

$$\{F_v\}=\begin{Bmatrix} k_{s1}(w_1+r_1)+c_{s1}\dot{w}_1+v\cdot c_{s1}\left(w_1'+r_1'\right) \\ k_{s2}(w_2+r_2)+c_{s2}\dot{w}_2+v\cdot c_{s2}\left(w_2'+r_2'\right) \\ k_{s3}(w_3+r_3)+c_{s3}\dot{w}_3+v\cdot c_{s3}\left(w_3'+r_3'\right) \\ k_{s4}(w_4+r_4)+c_{s4}\dot{w}_4+v\cdot c_{s4}\left(w_4'+r_4'\right) \\ 0 \\ 0 \end{Bmatrix} \quad \text{(A4)}$$

Youcef Khadri received his Magister and Ph.D from University of Badji Mokhtar, Annaba. He is currently a Assistant Professor in the Department of Mechanical Engineering, University Badji Mokhtar, B.P. 12 Annaba, Algeria. His research interests include vibration and dynamic systems, composite materials and vibratoire diagnosis of the machine failures.